02

Energy levels of the 603/700/787 nm luminescence system in natural diamond

© S.V. Lepekha[1], E.A. Vasilev[2], D.A. Zedgenizov[1,3], S.S. Savchenko[4], I.A. Wainstein[4]

[1] The Zavaritsky Institute of Geology and Geochemistry of Russian Academy of Sciences, Ekaterinburg, Russia
[2] St. Petersburg Mining University, St. Petersburg, Russia
[3] Ural State Mining University, Yekaterinburg, Russia
[4] NANOTECH Centre, Ural Federal University, Ekaterinburg, Russia

e-mail: Lepekha@igg.uran.ru

Received April 03, 2024
Revised June 03, 2024
Accepted June 28, 2024

A study was carried out of the photoluminescence system 603/700/787 nm in a natural diamond crystal at a temperature range of 77−300 K. In the emission spectra, two zero-phonon lines 584 and 603 nm appear at 300 K. Phonon replicas of about 40 and 70 meV assist the lines 656, 700 and 787 nm at 77 K. For the 603 nm zero-phonon line, one phonon replica of 69 meV is observed. The value of Huang-Rhys factor is 1.0, 1.2, and 0.7 for the corresponding lines 603, 700, and 787 nm: it indicates the middle level of the electron-phonon interaction. According to the excitation spectra, three exited energy levels were revealed: 2.86 eV for 656 and 700 nm, 2.68 eV for 584 and 603 nm, and 2.49 eV for 787 nm. The pairs of lines 584/603 and 656/700 nm can be interpreted as spin-allowed and forbidden electronic transitions, respectively.

Keywords: 603/700/787 nm system, diamond, photoluminescence, energy levels, phonon peaks, the Huang-Rhys factor.

DOI: 10.61011/EOS.2024.07.59645.6213-24

Introduction

Determination of optically active centers (OAC) in diamond is one of important applied spectroscopy areas. Despite the extensive research efforts, the nature of some diamond photoluminescence systems (PS) and OAC related to them has not been still understood. A set of 603 (2.054 eV), 700 (1.771 eV) and 787 nm (1.575 eV) lines that occurs only in natural diamond spectra is one of such systems. Pursuant to the study of quite constant intensity ratio 1 : 1.3 : 13 of zero-phonon line (ZPL) and similar optical properties, 603 nm, 700 nm and 787 nm ZPLs are commonly treated as a system [1–3]. The 603/700/787 nm system is observed in Ia type crystal spectra with nitrogen and hydrogen impurities [4]. The system is localized in the ⟨100⟩ [1,5,6] sectors characterized by higher (with respect to the ⟨111⟩ sectors) dislocation and hydrogen impurity content.

This system has been reported before as typical for natural diamonds with high share of A-form or B-form nitrogen defects and the presence of nickel centers S2 and 523 nm [2,4,5]. The study of man-made HPHT diamonds has shown that after annealing of Ni-containing crystals at 1950 K in the PL spectrum, 700.1 nm ZPL occurs with its intensity growing as the annealing temperature increases [7,8]. By such indirect indicators, the 603/700/787 nm system is assigned to Ni-containing centers. According to our data, this system frequently occurs in B-free crystals and is not associated with the presence of an elementary, but annealing-stable Ni atom in its interstitium position — the simplest defect with this element having the 883/885 nm ZPL in the PL spectrum.

Optical properties and temperature behavior of the 603 nm, 700 nm, 787 nm ZPL series are partially and discretely described in [1,4,8,9]. However, full-scale study and description of the system have not been performed yet. Thus, the nature of the 603/700/787 nm systems has not been reliably understood and its optical properties are underexplored. Meanwhile, the lines of this system are very intense in some natural crystals, and diamonds with this OAC may constitute a very promising optoelectronic material.

Samples and study methods

This study has investigated the optical properties of the 603/700/787 nm system using natural diamond crystal 123-76 from the Krasnovishersk District, Ural. The crystal was cut out and polished to a plate shape parallel to the {100} plane. The internal nonuniform structure and optical center distribution in crystal 123-76 have been discussed earlier

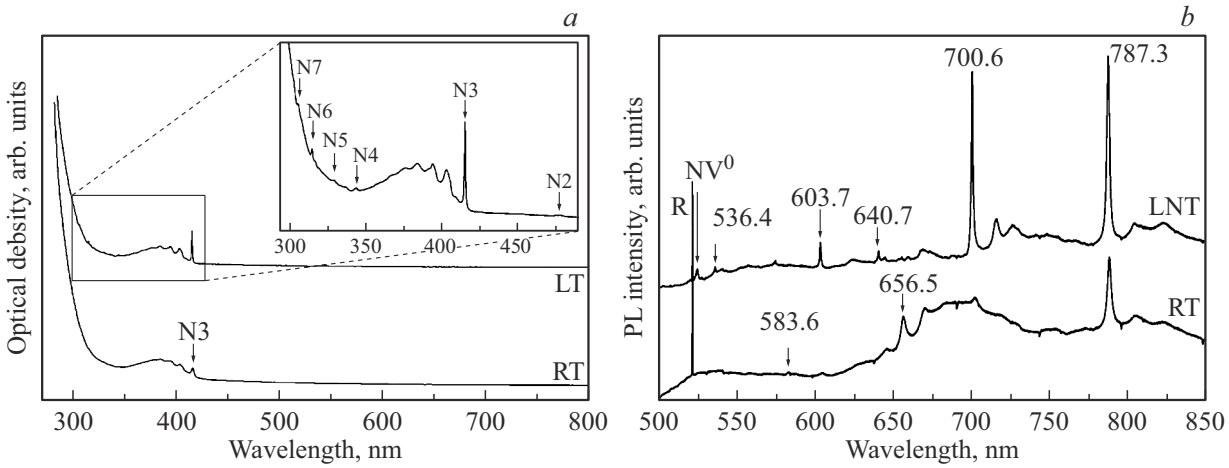

Figure 1. Absorption (*a*) and PL (*b*) spectra of the 123-76 plate at $T = 83$ K (liquid nitrogen boiling temperature, LNT), $T = 7$ K — LT and room temperature (RT). The PL spectra are recorded from one point in the ⟨100⟩ sector of the plate at $\lambda_{ex} = 488$ nm. The spectra are separated vertically for accuracy. R in the PL spectra means a Raman scattering (RS)line.

in [10,11]. According to the infrared (IR) spectroscopy, the total nitrogen impurity content varies from 800 ppm to 1400 ppm depending on the growth sectors. Nitrogen B-form prevails in sample 123-76 — about 67%. Nonuniform distribution of the N_3VH hydrogen center is observed — absorption coefficient of band 3107 cm^{-1} varies from 1.1 to 37.9 cm^{-1} in the ⟨111⟩ and ⟨100⟩ sectors, respectively.

PL spectra at 77 K and 293 K were recorded using the Horiba LabRAM HR800 Evolution spectrometer with the laser excitation $\lambda_{ex} = 488$, 514 and 633 nm and the Renishaw InVia spectrometer with the SSP-laser excitation $\lambda_{ex} = 787$ nm and LED source excitation $\lambda_{ex} = 360$ nm.

The 603 nm, 700 nm and 787 nm ZPL excitation spectra were recorded at 77 K, for the 584 nm and 656 nm lines — at room temperature using the Horiba FL3 spectrometer with lamp intensity correction.

The absorption spectra were analyzed at 296 K and 7 K using the Shimadzu UV-2450 spectrophotometer and a low-temperature measurement system. The sample temperature was controlled using a cryogenic system consisting of the CCS-100/204N closed-loop helium cryostat, Lake Shore Model 335 temperature controller, Sumitomo HC-4E1 compressor and Pfeiffer Vacuum HiCube 80 Eco turbopump station. Spectral slit width and sampling interval were 0.5 nm and 0.1 nm, respectively.

Findings and discussion

An N3 center spectrum with a well-known structure (N_3V) is clearly outlined in the absorption spectra of plate 123-76 at room temperature (Figure 1, *a*). OAC is also marked in the PL spectra for $\lambda_{ex} = 360$ nm (Figure 2, *a*). When the crystal is cooled to 7 K, the absorption spectrum contains, besides N3, an N2−N7-line series. N5, N6 and N7 lines are assigned to transitions on the A-center [12]. absorption on N4 and N2 is associated with electronic-vibrational transitions in the N3-center [12]. There are no absorption bands in the spectra in the wavelength range from 500 nm to 900 nm.

In the PL spectra at $\lambda_{ex} = 488$ nm, intensity of the 603/700/787 nm ZPL system is higher than that of other OAC (Figure 1, *b*). This feature is valid both for the ⟨111⟩ and ⟨100⟩ spectra. System intensity in the ⟨100⟩ sectors is at least 30 times higher than in ⟨111⟩. At room temperature, the intensity of 603 nm and 700 nm lines decreases to the maximum. The 583.6 nm and 656.5 nm ZPL occur in the spectrum (Figure 2, *b, c*). In [13], correlation of 701 nm and 656 nm ZPLs is reported according to their temperature dependences.

Besides the 603/700/787 nm system, the PL spectra for the ⟨100⟩ sectors have OAC associated with the nitrogen vacancy N3 and NV^0 crystal defects and nitrogen-nickel (523 nm and 793 nm) crystal defects (CD). An important feature of the 603/700/787 nm emission spectra at low temperatures is the presence of 793 nm ZPL at $\lambda_{ex} = 360$ and 633 nm that may be taken as phonon repetition (Figure 2, *a*). A wide PL band is also observed in the range 470−550 nm in the PL spectra recorded at 77 K and 297 K with 450 nm excitation.

The OAC and PL absorption spectroscopy data is shown in Table 1. Study of the man-made and natural diamond crystals with the Ni impurity by the EPR and PL spectroscopy methods in [7] was used to propose models in the form of the Ni ion in the divacancy position with three (NE2) and four (NE8) nitrogen atoms for the 523/NE2 nm and 793/NE8 nm centers.

The 603.7 nm (2.054 eV) ZPL emission spectrum has one 623.7 nm (1.986 eV) phonon peak with the interval between the zero-phonon transition and phonon repetition energies $\Delta E = 69 \pm 1$ meV (Figure 3, *a*). For the 700.6 nm (1.77 eV) line, the first phonon repetition peak is observed at 716.1 nm

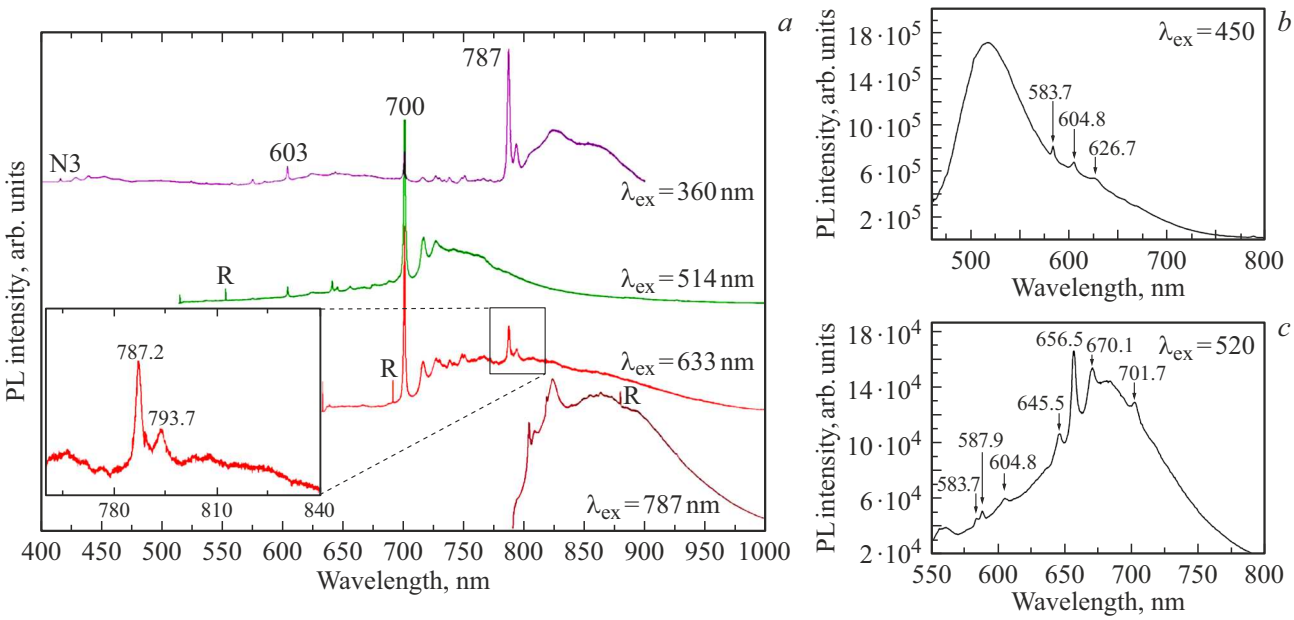

Figure 2. PL emission spectra at various excitation wavelengths and sample temperatures: $T \approx 83$ (a) and ≈ 300 K (b, c). R denotes the RS line.

Table 1. OAC in the absorption and PL spectra at low temperatures for plate 123-76

OAC in absorption spectrum, nm	PL centers				
	$\lambda_{ex} = 360$ nm	$\lambda_{ex} = 488$ nm	$\lambda_{ex} = 514$ nm	$\lambda_{ex} = 633$ nm	$\lambda_{ex} = 787$ nm
N7, N6, N5, N4, N3, N2	N3 523.5 536.2 543.8 557.3 560.1 NV^0 584.5 603.6 640.5 643.1 700.6 787 793.5	507.8 536.4 NV^0 603.7 640.7 655.6 700.6 787.3 925.7	NV^0 603.7 640.7 644.8 655.6 700.6 926.1	638.5 700.6 787.2 793.7	803.4 817.9 822.8 853.9 862.6 926

(1.731 eV) with $\Delta E_1 = 38 \pm 1$ meV, the second peak is observed at 726.6 nm (1.707 eV) with $\Delta E_2 = 63 \pm 1$ meV (Figure 3, b). The 787.2 nm (1.575 eV) ZPL phonon spectrum consists of two repetitions at 806.1 (1.538 eV) and 823.2 nm (1.506 eV) with $\Delta E_1 = 37 \pm 2$ meV and $\Delta E_2 = 69 \pm 1$ meV, respectively (Figure 3, c).

Phonon repetition in the PL spectrum with ~ 40 meV suggests that there is a vacancy in the arrangement of any CD diamond. A phonon repetition with an interval close to 70 meV may be assigned to the Λ_3(A) branch of the diamond's dispersion curves. Such phonon spectra structure is observed for the S2, S3, 523 and 793 nm systems that occur in natural and man-made crystals [1,7,8,14,15]. The proposed CD models for centers S2, S3, 523 and 793 nm have Ni in the divacancy positions and several N atoms[7].

The electron-phonon interaction force at low temperatures may be characterized by the dimensionless Huang–Phys factor [15–17]:

$$S = \ln \frac{I}{I_0},$$

where I_0 and I — are energy-integral luminescence intensities for ZPL and whole phonon spectrum, respectively. For the 603 nm electronic transition line, the Huang–Rhys factor is equal to $S = 1.0 \pm 0.1$. The 700 nm phononless line is characterized by $S = 1.2 \pm 0.3$, and the calculated factor for the 787 nm line is equal to $S = 0.7 \pm 0.3$. For ZPL assigned to Ni-containing CD, the Huang –Rhys factor varies from 0.4 to 3.5 [15–17], which characterizes the mean electron-phonon interaction force. For the GR1 (740.9 and 744.4 nm) centers representing an ordinary CD — a vacancy, the Huang–Rhys factor, by various estimates (3.7, 5.7 and 9.2), indicates a strong electron-phonon interaction [16]. For a substituent boron atom (2800 cm^{-1}) $S = 0.18 \pm 0.02$ and CD with a silicon atom (737.5 nm) $S = 0.24 \pm 0.02$, and the Huang–Rhys factor indicates a weak electron-lattice interaction [12].

The 603 nm PL line excitation spectrum (Figure 3, d) has a phononless transition peak 462.1 nm (2.683 eV) with a phonon wing to 390.9 nm (3.171 eV). At 700 nm, the excitation spectrum (Figure 3, e) has a different outline —

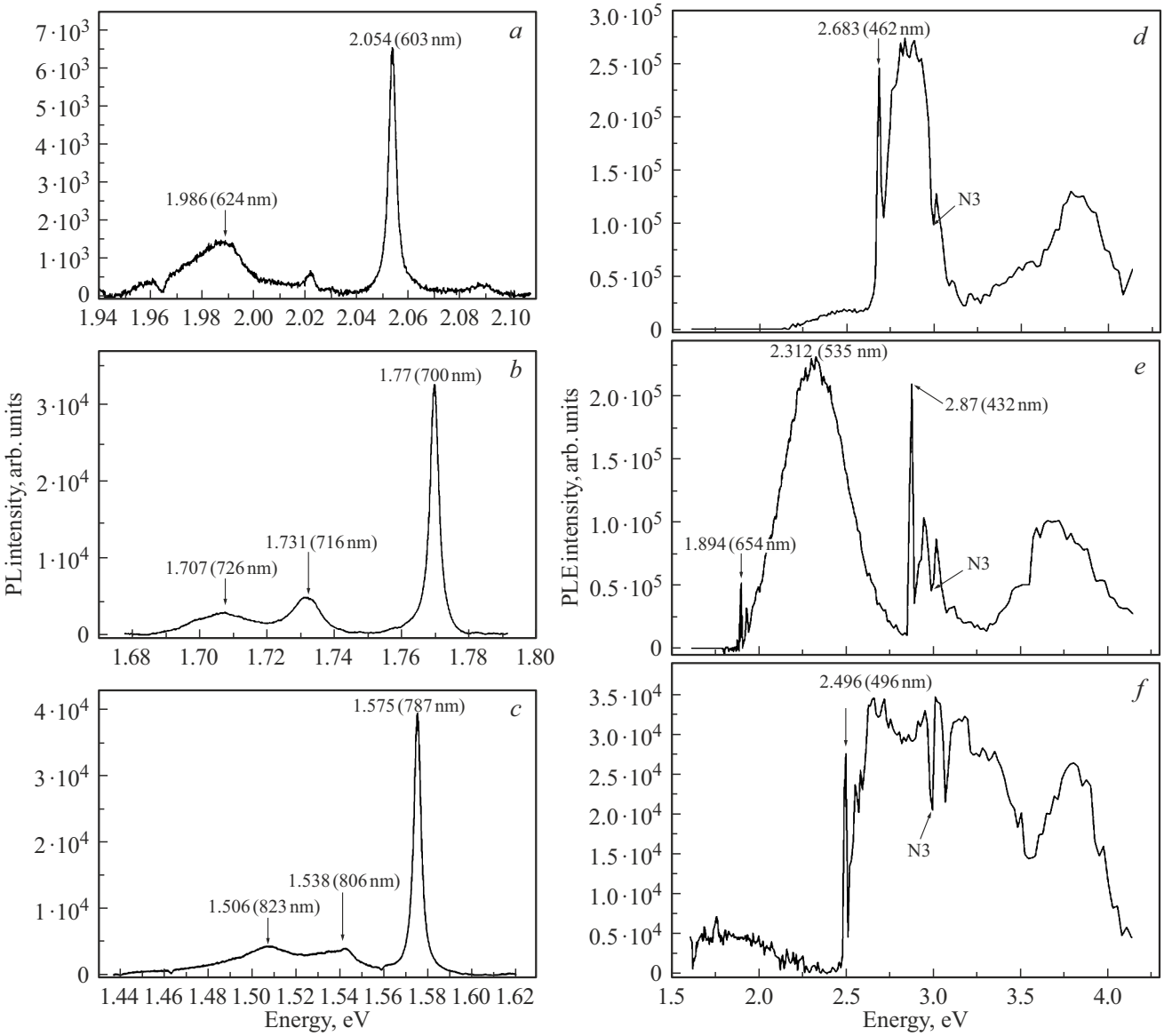

Figure 3. PL emission spectra (*a, b, c*) and excitation spectra (*d, e, f*) for 603 (*a, d*), 700 (*b, e*) and 787 nm (*c, f*) lines. $T \approx 77$ K.

two phononless lines at 431.9 nm (2.87 eV) and 654.5 nm (1.894 eV) and a wide peak near 535 nm (2.312 eV). A phononless transition in the excitation spectrum for the 787 nm line is highlighted at 496.7 nm (2.496 eV). For all excitation spectra, there is a reabsorption band at 415.2 nm (2.986 eV) associated with the N3 center.

At room temperature, 603 nm ZPL in the PL spectra looses its intensity, broadens and shifts to the red spectrum region up to 604.8 nm (Figure 4, *a*). Behavior of the 603 nm center phonon wing is similar to the electronic transition line — broadening, reduced line intensity and shift to the long-wavelength region up to 626.7 nm are observed. A faint 584 nm line occurs in the PL spectrum at the same time. The 584 nm line excitation spectrum (Figure 4, *c*) has 462 (2.682 eV) nm ZPL with a phonon wing up to 400 nm (3.1 eV).

As mentioned above, 656.6 nm ZPL with two phonon repetitions 670.1 nm (1.85 eV) and 683 nm (1.815 eV) with the intervals between phononless transition and phonon repetition energies $\Delta E_1 = 38 \pm 2$ meV and $\Delta E_2 = 73 \pm 2$ meV, respectively, occurs in the PL spectra at $T \approx 300$ K (Figure 4, *b*). The 656 nm line excitation spectrum has 434 (2.857 eV) ZPL with a phonon wing up to 400 nm (3.1 eV). In the 584 nm and 656 nm line excitation spectra, there is a reabsorption band at 415.2 nm (2.986 eV) associated with the N3 center.

In accordance with the PL excitation spectra, the 603/700/787 nm system emission spectra at various source excitation wavelengths have a different shape at 297 K and 77 K.

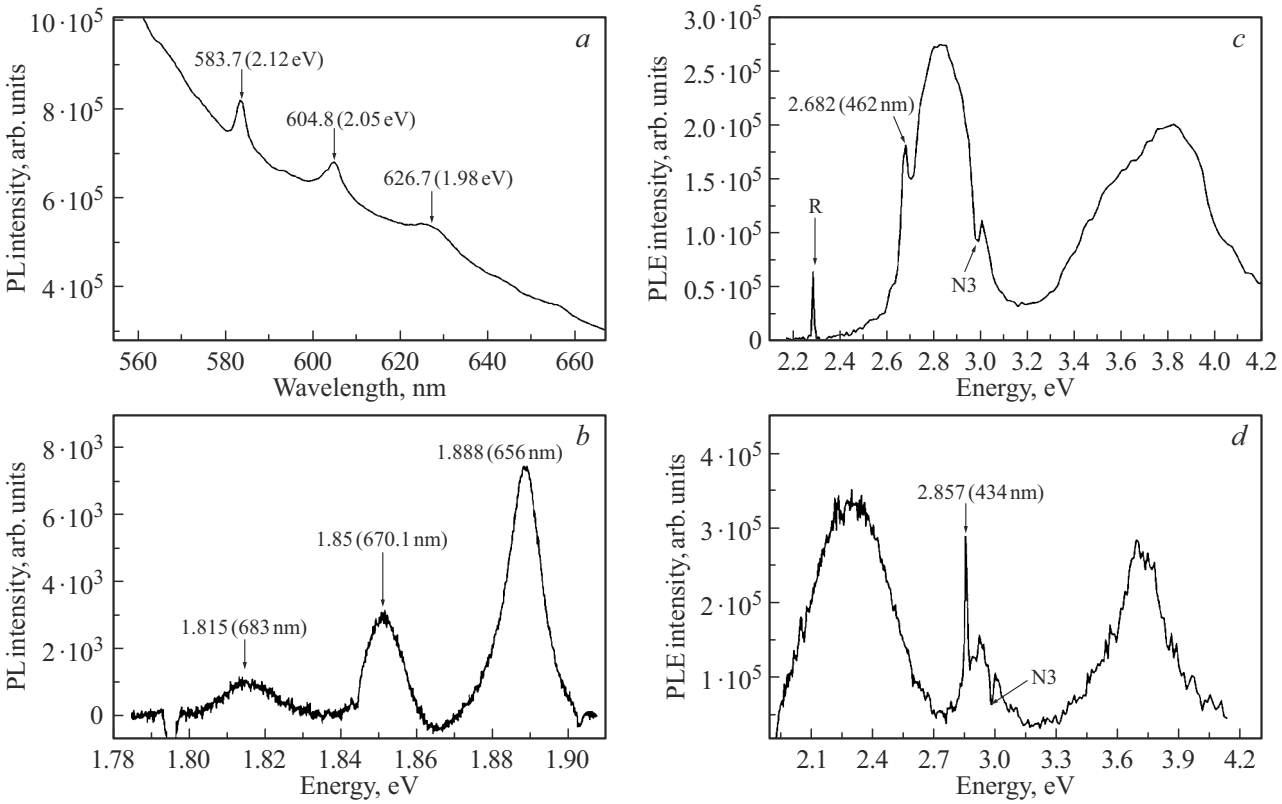

Figure 4. PL emission spectra (*a, b, c*) and excitation spectra (*c, d*) for 584 (*a, c*) and 656 (*b, f*) lines. $T \approx 300$ K. R denotes the RS line.

Table 2. Features of the 603/700/787 nm system emission and excitation spectra

λ_{pl}, nm	E_{pl}, eV	FWHM, meV	ΔE Reference, meV	S	E_{ple}, eV	
603.7	2.054	3.3	69 ± 1	1.0 ± 0.1	2.683	
700.6	1.77	3	38 ± 1 63 ± 1	1.2 ± 0.3	2.87 1.894 2.312	
787.2	1.575	3.8	37 ± 2 69 ± 1	0.7 ± 0.3	2.496	this
583.7	2.124	5.4	–	–	2.682	study
656.6	1.888	8.7	38 ± 2 73 ± 2	–	2.857	
603.8	2.053	–	∼ 70	–	–	
700	1.771	–	∼ 40	–	330, 450	[1]
788%	1.573	–	∼ 40	–		
603.5	2.055	–	33 90	–		
700.3	1.771	–	40 60	–		[4]
786.6	1.576	–	–	–		
700.5	1.770	3.4	63 120 175	–	–	[9]
787.1	1.575	4.6	38 94 141	–	–	
700.1	1.771	–	18	–	–	[8]

The features of the 603/700/787 nm system phonon spectra and excitation spectra are summarized in Table 2. For comparison, Table 2 is supplemented by the literature data.

The 656 nm and 700 nm line excitation spectra have the same shape and a common ZPL with 2.86 eV and a wide peak at about 2.312 eV. The correlation between the 656 nm and 700 nm electronic transitions is also indicated by the phonon repetition structure in the emission spectra.

The 584 nm and 603 nm system line have the same similarity. Their excitation spectra have a common ZPL with 2.682 eV. Supposing that the 584 nm ZPL phonon

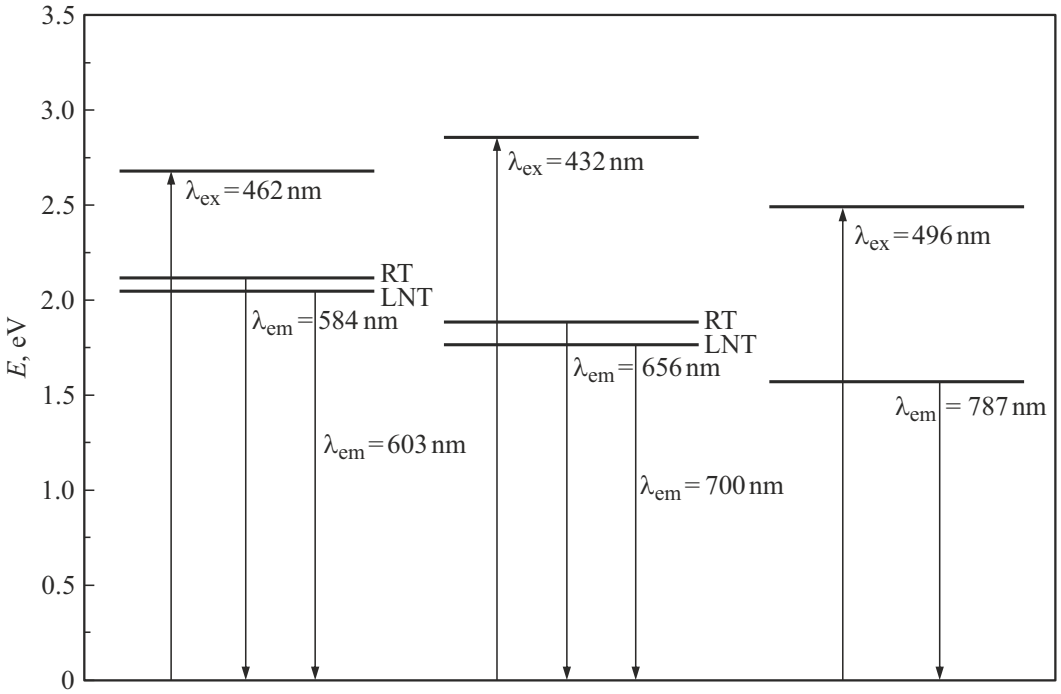

Figure 5. 603/700/787 nm system energy level and quantum transition diagram.

spectrum structure contains one phonon repetition with $\Delta E \approx 69$ meV (similar to 603 nm ZPL), then occurrence of this repetition shall be expected in the emission spectrum with 2.055 eV (603.3 nm) at the wide 604.8 nm ZPL. Thus, the absence of the observed phonon repetitions of 584 nm in the emission spectrum is attributable to imposition on 603 nm ZPL.

The features of 584/603 nm and 656/700 nm ZPLs (Figure 5) are simil the S3 (N_2NiV_2) system shown in [18], where two radiative transitions are observed — spin-allowed 2.621 eV (473 nm) at $T = 70$ K and spin-forbidden 2.496 eV (496 nm) at $T = 170$ K with the level energy difference 125 meV. In the 603/700/787 nm system, the difference between resistive levels 1.888 eV (656 nm) and 1.77 eV (700 nm) is 118 meV. For emissive levels 2.124 eV (584 nm) and 2.054 eV (603 nm), the difference is equal to 66 meV. Further study of the 603/700/787 nm system decay kinetics and temperature dependences is expected to prove the supposed spin-forbidden transition model for 603 nm and 700 nm ZPLs typical of the *d*-element impurity.

The provided 603/700/787 nm system energy level diagram, electron-phonon interaction force and expected spin-forbidden PL transition mechanism are similar to OAC based on Ni-N CD (S2, S3, 523 and 793 nm). However, according to our data, the system often occurs in natural crystals without B-centers and is not associated with the presence of interstitial Ni atoms that are stable in annealing and have 883/885 nm ZPL in the PL spectrum. Moreover, the 787 nm ZPL intensity distribution maps for the three studied crystals are consistent with the 3107 cm^{-1} hydrogen center intensity distribution maps. Thus, it can be concluded that the 603/700/787 nm PL system is defined by complex CD that involves Ni and H.

Conclusion

The 603/700/787 nm PL system has five phononless radiative transitions with 2.124 eV, 2.054 eV, 1.888 eV, 1.77 eV and 1.575 eV levels. The first two 2.124 eV and 2.054 eV transitions originate from the same excited 2.68 eV level and may be interpreted as spin-forbidden 2.054 eV and spin-allowed 2.124 eV transitions. Similar behavior is observed for the pair of 1.888 eV and 1.77 eV transitions with the excited 2.86 eV level. The radiative 1.575 eV transition originates from the excited 2.496 eV level and probably has a different luminescence mechanism. The findings suggest that it is important to study temperature dependences and decay kinetics of the 603/700/787 nm system.

Acknowledgments

The study was performed under topic № 123011800012-9 of the state assignment of the Institute of Geology and Geochemistry, Ural Branch of the Russian Academy of Sciences and grant 21-77-20026 provided by the Russian Science Foundation. I.A. Vainshtein and S.S. Savchenko are grateful for support to the M.V. Maksimov and A.M. Nadtochii acknowledge support from the project FEUZ-2023-0014.

Absorption spectra were measured at NANOTECH Research and Education Center, Ural Federal University. Some PL spectra were recorded using the equipment provided by Geoanalitik Shared Research Facility, Institute of Geology and Geochemistry, Ural Branch of the Russian Academy of Sciences. Excitation and emission spectra are recorded the LIVS Shared Research Facility, Saint-Petersburg Mining University.

Conflict of interest

The authors declare that they have no conflict of interest.

References

[1] S.P. Plotnikova, Yu.A. Klyuev, I.A. Parfianovich. Min. zhurn. **2** (4), 75 (1980) (in Russian).
[2] L. Tretiakova. Eur. J. Mineral., **21**, 43 (2009). DOI: 10.1127/0935-1221/2009/0021-1885
[3] G.B. Bokiy, G.N. Bezrukov, Yu.A. Kluev, A.M. Naletov, V.I. Nepesha. *Prirodnye sinteticheskie almazy* (Nauka, M., 1986) (in Russian).
[4] K. Iakoubovskii, G.J. Adriaenssens. Diamond Relat. Mater., **11** (1), 125 (2002). DOI: 10.1016/S0925-9635(01)00533-7
[5] A.R. Lang, A.P. Yelisseyev, N.P. Pokhilenko, J.W. Steeds, A. Wotherspoon. J. Cryst. Growth., **263** (1), 575 (2004). DOI: 10.1016/j.jcrysgro.2003.11.116
[6] A.R. Lang, G.P. Bulanova, D. Fisher, S. Furkert, A. Sarua. J. Cryst. Growth., **309** (2), 170 (2007). DOI: 10.1016/j.jcrysgro.2007.09.022
[7] V.A. Nadolinny, A.P. Yelisseyev, J.M. Baker, M.E. Newton, D.J. Twitchen, S.C. Lawson, O.P. Yuryeva, B.N. Feigelson. J. Phys.: Condens. Matter, **11** (38), 7357 (1999). DOI: 10.1088/0953-8984/11/38/314
[8] A. Yelisseyev, V. Nadolinny, B. Feigelson, Y. Babich. Int. J. Mod. Phys. B, **16** (6), 900 (2002). DOI: 10.1142/S0217979202010580
[9] Y.K. Vohra, C.A. Vanderborgh, S. Desgreniers, A.L. Ruoff. Phys. Rev. B, **39** (8), 5464 (1989). DOI: 10.1103/PhysRevB.39.5464
[10] E.A. Vasiliev, I.V. Klepikov, I.V. Antonov. Zapiski RMO, **147** (4), 126 (2018) (in Russian). DOI: 10.30695/zrmo/2018.1474.10
[11] E.A. Vasilev. In: *XIII General Meeting of the Russian Mineralogical Society and the Fedorov Session. GMRMS 2021. Springer Proceedings in Earth and Environmental Sciences*, ed. by Y. Marin (Springer, Cham, 2021), p. 597. DOI: 10.1007/978-3-031-23390-6_75
[12] A.M. Zaitsev. *Optical properties of diamond: a data handbook* (Springer-Verlag, Berlin, 2001).
[13] F.A. Stepanov, A.S. Emelyanova, A.L. Rakevich, E.F. Martynovich, V.P. Mironov. Izv. RAN. Ser. fiz., **83** (3), 371 (2019) (in Russian). DOI: 10.1134/S0367676519030232
[14] E.V. Iliin, E.V. Sobolev, O.P. Yurieva. FTT, **12** (7), 2223 (1970) (in Russian).
[15] I.N. Kupriyanov, V.A. Gusev, Yu.M. Borzdov, A.A. Kalinin, Yu.N. Pal'yanov. Diamond Relat. Mater., **8** (7), 1301 (1999). DOI: 10.1016/S0925-9635(99)00122-3
[16] J. Walker. Rep. Prog. Phys., **42** (10), 1605 (1979). DOI: 10.1088/0034-4885/42/10/001
[17] E.F. Martynovich, V.M. Sapozhnikov. Opt. i spektr., **48**, 1221 (1980) (in Russian).
[18] E. Pereira, L. Santos. J. Lumin., **45**, 454 (1990).

Translated by E.Ilinskaya